MICROSCOPY RESEARCH AND TECHNIQUE 30:480–490 (1995)

Mapping of the Orientation of Myocardial Cells by Means of Polarized Light and Confocal Scanning Laser Microscopy

PIERRE-SIMON JOUK, YVES USSON, GABRIELLE MICHALOWICZ, AND FRANCK PARAZZA
Equipe de Reconnaissance des Formes et de Microscopie Quantitative, CERMO (P.-S.J., Y.U., F.P.), and Service de Medecine Néonatale, Centre Hospitalier Universitaire de Grenoble (P.-S.J., G.M.), Université Joseph Fourier, BP 217, 38043 Grenoble Cedex 9, France

KEY WORDS Multiparametric image analysis, Heart, Myocardium, Fetus, Neonatal

ABSTRACT The study of the topological organisation of myocardial cells is a basic requirement for the understanding of the mechanical design of the normal and pathological heart. We developed a technique based on multiparametric image analysis of transmitted polarized light to generate maps of the azimuth and the elevation angles of the myocardial cells. The properties of birefringence of the myocardium embedded in methylmetacrylate were measured in papillary muscles with monitored 3D orientation. This birefringence is positive uniaxial with a 0° extinction angle when the axis of the fiber is parallel to the axis of the polarizer or the analyzer. Thick sections were studied between crossed polars, and four images of each section were digitized for an angle of the polarizer with the section varying from 0–67.5° in steps of 22.5°. The amounts of transmitted light for each setup of the polarizer were combined in order to extract the values of the azimuth angle (modulo 90°) and the elevation angle of the myocardial cells, according to the Johannsen equation. The respective maps of these angles were calculated and then assessed with confocal scanning laser microscopy. This method provides an efficient and accurate tool for the study of the histological architecture of the fetal and neonatal heart.

INTRODUCTION

The topological organisation of cardiac myofibres in fetal and neonatal hearts depends on two factors: the migration of the embryonic cardiac compounds during morphogenesis and mechanical stress developed in fetal ventricular walls. Knowledge of this organisation is a basic requirement for understanding the mechanical design of the normal and pathologic fetal and neonatal heart.

The adult ventricular myocardium is a muscle made of a three-dimensional network of myocardial cells connected by anastomoses (Fox and Hutchins, 1972). This network or connection pattern is highly structured and was described as a multilayered organisation where each layer of myocardial cells has a preferred orientation (Streeter, 1979). This pattern has been studied with three different approaches: mechanical peeling of the fibres of the total heart from epicardium to endocardium (Greenbaum et al., 1981; Torrent-Guasp, 1973), study of macroscopical serial sections of the heart (Hort, 1960), and histological study of sampled region of myocardium of the ventricular wall (Streeter, 1979). In pathology, different methods of investigating the organisation of myocardial fibres have been developed at the macroscopic and microscopic levels. These were based mainly on semiautomatic quantitative techniques (Maron and Roberts, 1978, 1979a,b, 1981; McLean and Prothero, 1987, 1991) where an operator draws the main axis of the in-plane fibres on a digitizer tablet. A different and more sophisticated technique has been used by Whittaker et al. (1989) and Pickering and Boughner(1990). The thin sections were observed by polarized light microscopy. Muscle cells were selected on a stereological grid, and then the stage of the microscope was rotated until the cells were at extinction. The extinction angle was recorded as the cell orientation angle. However, although these techniques provide information on the azimuth angle in the plane of the section, they lack information on the obliquity of fibres (i.e., the elevation angle).

In this paper we present an original approach to characterize the orientation of myocardial cells. We developed a multiparametric image analysis programme using polarized light microscopy in order to obtain a three-dimensional map of the myofibre orientations at the histological and anatomical level. The principle of the method is to use the uniaxial polarizing properties of myocardium. This method was assessed by 3D imaging of the nuclei of the myocardial cells in fluorescence using confocal scanning laser microscopy (CSLM).

MATERIALS AND METHODS

Human Fetal Hearts

Human fetal hearts (14–40 weeks of gestational age) were fixed in a solution of 10% neutral buffered formalin by perfusion. They were then immersed 1 week in the same solution.

Address reprint requests to P.-S. Jouk, Service de Medecine Neonatale, Centre Hospitalier Universitaire de Grenoble, Université Joseph Fourier, BP 217, 38043 Grenoble Cedex 9, France.

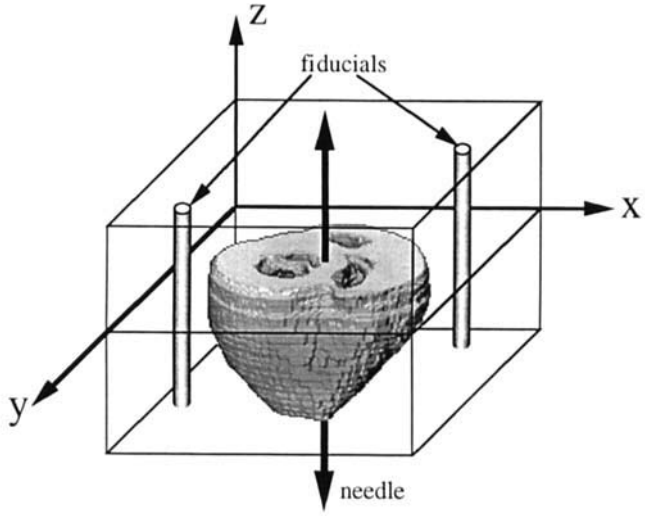

Fig. 1. Orientation of the heart during the polymerization process. The y axis is parallel to the interventricular septum. The z axis runs along the baso-apical axis of the heart and is parallel to the optical axis of the microscope.

Histological Preparation

Embedding. The hearts were embedded in a resin of methyl methacrylate (MMA) using the following protocol. The specimens were infiltrated at room temperature with two solutions of glycol methacrylate (GMA) in water with increasing concentration (1 week each) followed by immersion in pure GMA for 1 week. They were then infiltrated for 1 week in a series of mixtures of GMA and MMA in which the concentration of MMA was gradually increased to end with pure MMA. The hearts were embedded by polymerization of MMA at a temperature of 32°C.

Fiducials. In order to have a constant anatomical reference for further orientation analysis, the hearts were maintained vertically during the polymerization process. This was obtained by transfixation with a thin needle along a baso-apical axis of the heart. After polymerization, four holes (block fiducials, diameter 1 mm) were drilled in the embedding resin at constantly registered positions with their axes parallel to the baso-apical axis of the heart. The reference system for the three-dimensional space was defined as follows: the xy plane corresponds to the section plane with the y axis parallel to the interventricular septum, and the z axis is aligned with the baso-apical axis of the heart (Fig. 1).

Sectioning. For every heart, a series of thick sections (500 μm) was cut with a rotatory microtome (1600; Leica). The rate of penetration of the rotory saw was set to a low speed (15 min per section) in order to avoid mechanical stress and distortions.

Staining. After examination by polarized light microscopy some selected sections were stained with Feulgen for confocal scanning laser microscopy. Staining was performed on the sections prior to mounting them on glass slides. This insures that the solutions penetrate the thick sections by their two sides, giving an in-depth staining. Because the sections were not deplastified they were highly hydrophobic, and it was necessary to permeabilize them with a solution of 20% tetrahydrofurane (THF) in water. After hydrolysis in HCl 6 N for 2 h at room temperature, the sections were rinsed in water and left in Schiff reagent for 4 h at room temperature. They were then left in four baths of bisulfite water 0.5% for 10 min each and rinsed in water. After staining, the sections were laid on glass slides in a 20% solution of THF to help them spread. After 2 h, the slides were rinsed in water and mounted with an anti-fading solution under coverslips.

Polarized Light Microscopy

Prior to staining, the thick sections were analyzed with a SV11 stereomicroscope (Zeiss) equipped for polarized light with a strain birefringence free objective (×0.6) and crossed polarizer and analyzer. In order to answer both requirements, examination with polarized light and videomicroscopy with multiparametric acquisition, we designed a new stage microscope. In this stage the specimen stage is fixed, and the crossed polarizer and analyzer can rotate. The section was always placed with its x axis running along the east-west axis of the specimen stage. Images were recorded with a black-and-white CCD video camera interfaced with a SAMBA 2005 (Alcatel-TITN) image processing and analysis system. The CCD videocamera (Burle) was used as a photometric detector after we checked that the grey level was a linear function of the light intensity. The intensity of the white light of the illuminator (Schott) was adjusted in order that a retardation of 50 nm given by a calibrated mica plate at 45° of the east-west axis of the stage corresponded to the maximum grey level 255. Four images per section were recorded and digitized for four different angles α (0°, −22°5, −45°, −67°5) of the polarizer with reference to the x axis of the section which stay fixed on the specimen stage (Fig. 2).

The amount of monochromatic light that reaches the upper polar, always crossed with the lower polar and allowed to pass through, is given by (Johanssen, 1918):

$$\frac{I}{I_0} = \sin^2 \pi \frac{\Delta}{\lambda} \times \sin^2 2\tau \qquad (1)$$

where Δ and λ are the retardation and wavelength of the monochromatic light, respectively, τ is the angle between the direction of the fibre and the closest direction of the polarizer or the analyzer, and I_0 is the intensity of light with no retardation. The birefringence of unstained biological molecules is weak, so the retardation is always less than half the shortest wavelength of light (i.e., 200 nm). This condition makes it possible to use white light instead of monochromatic. In this case the amount of light that reaches the upper polar also depends on the spectrum of emitted light and the response of the camera to the different wavelengths. This has to be calibrated for each optical system. Our system responds as a system illuminated with a 590 nm monochromatic light: λm. Another consequence of

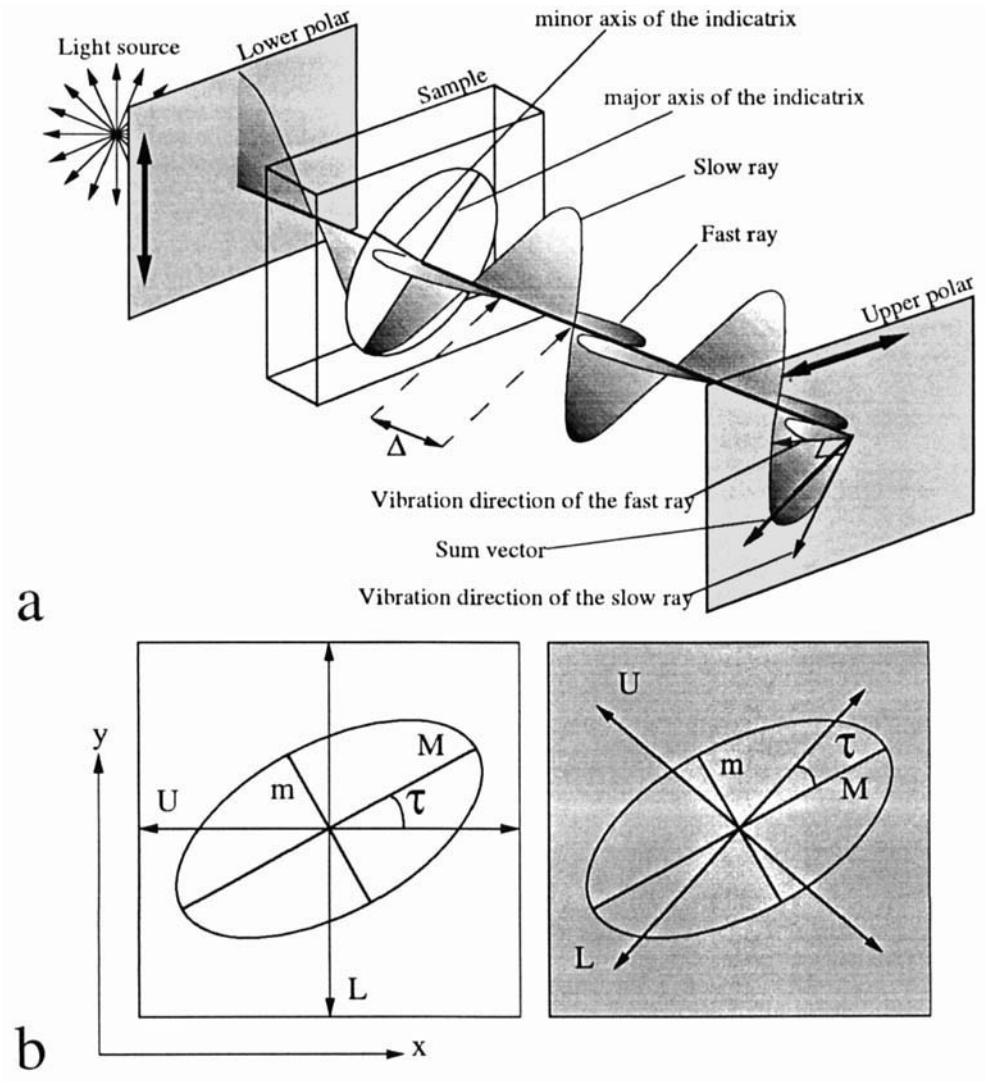

Fig. 2. **a:** Schematic view of the development of a path difference when a light ray traverses a birefringent sample. The linearly polarized light ray, whose vibration direction is defined by the axis of the lower polar, entering the sample is split into slow and fast rays. While the slow ray passes through the sample, the fast ray travels through the mineral plus an additional distance Δ, which is the retardation. The vector components of the two rays sum at the upper polar. **b:** The amount of light that is allowed to get through the upper polar is proportional to the square sine of 2τ, where τ is the closest angle between the vibration direction of the slow (M) or fast ray (m) and the axis of the lower (L) or upper polar (U). On the left, the value of τ is larger than on the right, and the amount of transmitted light is larger.

this weak birefringence is that the retardation is always lower than half the wavelength of the light. In this interval the first term of the Johansenn equation is a function of I/Io that will allow us to extract the angular information by measuring the amount of transmitted light. While the second term of the equation varies like the sine of 2τ, the azimuth information will be known only as modulo 90°.

Since a CCD camera was used as a photometric detector, this equation can be written

$$\frac{L}{L_0} = \sin^2 \pi \frac{\Delta}{\lambda} \times \sin^2 2\tau \qquad (2)$$

where L is the measured gray level for a given sample and L_0 is the gray level when there is no retardation and the polarizer is parallel to the analyzer. Because the system was calibrated to insure that a 50 nm retardation corresponds to the maximum grey level of 255, L_0 was out of range of the measured L and had to be calculated by extrapolation:

$$L_0 = \frac{255}{\sin^2 \frac{50\pi}{590}} = 3{,}684. \qquad (3)$$

Measurement of the Maximum Birefringence of the Myocardium. The retardation is a function of the thickness and birefringence of the sample:

$$\Delta = d(n_s - n_f) \tag{4}$$

where d is the thickness of the sample, the term $(n_s - n_f)$ is the birefringence of the sample, and n_s and n_f are the indices of refraction for the slow and the fast ray, respectively. The birefringent molecules of the myocardium, myosin and collagen, are both optically positive uniaxial molecules (Wolman, 1975), so that the maximum birefringence is created by the molecules which lie in the plane of the slide (i.e., the coplanar fibres), perpendicular to the optical axis of the stereomicroscope. The maximum amount of light that reaches the upper polar and the CCD camera is transmitted by the coplanar fibers with a τ angle of 45°. The measurement of maximum intensity transmitted by the sample L_{max} permits calculation of the maximum birefringence of the sample according to equations 1 and 2:

$$(n_s - n_f)_{\max} = \frac{\lambda m}{d \times \pi} \sin^{-1} \sqrt{\frac{L_{\max}}{L_0}}. \tag{5}$$

The range of maximum birefringence value $(n_s - n_f)_{\max}$ observed in 21 hearts weighing between 1.5 and 16 g and prepared as described above was 0.6 10^{-4} to 10^{-4}. These low values are close to the crystal birefringence of myosin (Taylor, 1975). The value of the refractive index of methylmetacrylate 1.4121 is close to the value of refringence of proteins. This dims the form birefringence which is of lesser interest for the study of the three-dimensional orientation of molecules (Frey-Wyssling 1957; Ruthman 1970).

Theoretical Model. Before any attempt to extract the information on the orientation of myocardial fibres, it is necessary to characterize the optical properties of our material in polarized light. This was done using the pillars of the atrioventricular valves, whose spatial orientation is known. As we shall demonstrate later, fetal and neonatal myocardium embedded in methylmetacrylate reacts between crossed polars as a crystal whose indicatrix is positive uniaxial with a 0° extinction angle. The amount of transmitted light for a heart of known maximal birefringence is a function of the three-dimensional orientation of the main axis of its indicatrix. This orientation can be decomposed into two angles: the azimuth angle Φ, the angle of the projection of the major or the minor axis of the indicatrix on the xy plane of the section with the east-west axis of the optical system, and the elevation angle Θ, which is the angle of the indicatrix with the xy plane. The purpose of this short review will be to consider, from a theoretical point of view, how the orientation information of a sample ought to be extracted when primary optical properties are known.

As we have previously seen, the amount of transmitted light is a function of the τ angle. This angle is itself a function of the angles Φ and α. τ is the minimum value of $\Phi \pm \alpha$. Thus, for a given setup of the α angle and for a given value of the retardation Δ (i.e., known birefringence and thickness of the sample), the amount of transmitted light is a function of Φ:

$$\frac{L}{L_0} = \sin^2 \pi \frac{\Delta}{\lambda_m} \times \sin^2 (2 \times \min\{\Phi - \alpha, \Phi + \alpha\}). \tag{6}$$

This function where $\min\{\Phi - \alpha, \Phi + \alpha\}$ is the smallest value of the set $\{\Phi - \alpha, \Phi + \alpha\}$ and gives the azimuth angle Φ modulo $\Pi/2$.

The birefringence of the myocardium is a function of the elevation angle Θ (Phillips, 1971):

$$(n_s - n_f) = n_f \times \left(\frac{1}{\sqrt{1 + \left(\frac{{n_f}^2}{{n_{s\max}}^2} - 1 \right) \cos^2 \theta}} - 1 \right). \tag{7}$$

In biological tissues, the values of the refractive indices n_f varies between 1.4 and 1.6. Because of the large difference between $(n_s - n_f)_{\max}$ and n_f, the calculated birefringence does not vary significantly for values of n_f in the biological range, and equation 7 can be simplified as

$$(n_s - n_f) = 1.5 \left(\frac{1}{\sqrt{1 - \frac{2(n_s - n_f)_{\max} \cos^2 \theta}{1.5}}} - 1 \right). \tag{8}$$

The origin of the birefringence is probably composite, due to the myosin filaments of the sarcoplasm and to endomysial collagen, but the birefringence of the components sums up. Therefore, we are solely interested in the resultant and will always consider the global indicatrix of the myocardium.

Image Analysis. Our goal was to define the Θ and the Φ angles of the myocardial fibres by measuring the amount of transmitted light of every pixel of the digitized image of a whole slice of heart. For a given maximum birefringence of the myocardium, the amount of transmitted light is a function of two angles. Thus, in order to define them, it is necessary to resort to multiparametric acquisition. After image acquisition of the section and for every pixel, we have four measurements: $L\alpha_0$, $L\alpha_{22.5}$, $L\alpha_{45}$, $L\alpha_{67.5}$ (values of the measured grey level for a value of the α angle of 0°, 22.5°, 45°, and 67.5°, respectively). The difference between $L\alpha_{45}$ and $L\alpha_0$ varies as the cosine of 4Φ, and the difference between $L\alpha_{22.5}$ and $L\alpha_{67.5}$ varies as the sine of 4Φ. Thus $(L\alpha_0 - L\alpha_{45})$ and $(L\alpha_{67.5} - L\alpha_{22.5})$ are the two components of an imaginary number Z:

$$Z = (L\alpha_0 - L\alpha_{45}) + i(L\alpha_{67.5} - L\alpha_{22.5}) \tag{9}$$

and the value of the azimuth angle Φ modulo $\pi/2$ is

$$\Phi = \frac{1}{4} Arg(Z). \tag{10}$$

To calculate the elevation angle Θ it is necessary to consider the maximum value $L\alpha_{max}$ of $L\alpha_0$, $L\alpha_{22.5}$, $L\alpha_{45}$, $L\alpha_{67.5}$. For this value

$$\tau = \frac{\pi}{4} + \varepsilon \quad \text{with } \varepsilon \in \left[-\frac{\pi}{16}, +\frac{\pi}{16} \right]. \tag{11}$$

This term ε is a consequence of the π/8 gap between successive values of α. These discrete values approximate the optimal π/4 value of τ by only ±π/16. Thus ε = Φ mod π/16 if Φ mod π/8 < π/16 and ε = Φ mod π/16 − π/8 if Φ mod π/8 > π/16. Therefore, the birefringence of the myocardium is

$$(n_s - n_f) = \frac{\lambda m}{\pi d} \sin^{-1}\left(\frac{1}{\cos 2\varepsilon} \sqrt{\frac{L\alpha_{max}}{L_0}} \right). \tag{12}$$

According to equations 8 and 12, the value of angle Θ is

$$\theta = \cos^{-1} \sqrt{\frac{1.5((n_s - n_f)^2 + 3(n_s - n_f))}{2(n_s - n_f)_{max}((n_s - n_f) + 1.5)^2}}. \tag{13}$$

Because of the low values of $(n_s - n_f)$, this can be simplified as

$$\theta = \cos^{-1} \sqrt{\frac{(n_s - n_f)}{(n_s - n_f)_{max}}} \tag{14}$$

and in term of grey level values

$$\theta = \cos^{-1} \sqrt{\frac{\sin^{-1} \sqrt{\frac{L\alpha_{max}}{L_0}}}{\sin^{-1} \sqrt{\frac{L_{max}}{L_0}}}}. \tag{15}$$

Confocal Scanning Laser Microscopy

Developmental studies have shown that the nuclei of the skeletal muscle cells are elongated ovoids distributed almost regularly along the fibres "like a pearl necklace" (Harris et al., 1989). This particular shape of the nuclei and their regular distribution along the fibre can be exploited. Thus, the nuclei can be considered as good estimates of the fibre orientation. Selected zones of the Feulgen stained slides were investigated with a confocal scanning laser microscope LSM10 (Zeiss, Oberkochen, Germany). Fluorescence of the Feulgen dye was obtained using a helium-neon laser with an excitation wavelength of 543 nm. Emitted light was collected through an oil immersion objective lens 40×, N.A. 1.3 (Planapo Neofluar; Zeiss) and transmitted to the photomultiplier through a low-pass filter with a cutoff wavelength of 590 nm. The voxels were sampled every 0.47 μm in the in focus plane, and the microscope stage was lifted 0.47 μm between the recording of each optical section. Each optical section was recorded eight times for image averaging. The sections were stored as a series of 200 digital images (256 × 256 pixels) corresponding to a final volume of 120 μm by 120 μm by 95 μm representing a final amount of 13 Mbytes of data.

Three-Dimensional Image Analysis. The three-dimensional analysis and reconstruction programmes were written by the authors in C language on an Iris Indigo Entry (Silicon Graphics, Mountain View, CA). Some of the algorithms have been already described by Parazza et al. (1993).

Feature Extraction. The calculation of the mean orientation of a nucleus was based on the fitting of an ellipsoid to the shape of the nucleus (Usson et al., 1994). The orientation of a nucleus was expressed by means of a vector with unit length. The statistical information for a block of tissue was obtained by calculating the vectorial sum of all the nuclear unit vectors. The final result was expressed in terms of a mean azimuth angle Φ corresponding to the mean orientation of the projections of the nuclear orientations on the section plane, and a mean elevation angle Θ corresponding to the obliquity of nuclear orientations with reference to the section plane. The homogeneity of the nuclear orientation was given by the value of the modulus of the vectorial sum of all the nuclear unit vectors divided by the number of vectors (Batschelet, 1981).

RESULTS

Validation of the Theoretical Model

The theoretical model is based on the hypothesis that the indicatrix of the myocardium embedded in methylmetacrylate is positive uniaxial with a 0° extinction angle.

This model was assessed by measuring the amount of transmitted light of biological samples with monitored Θ and Φ angles. Papillary muscles of fetal and neonatal hearts were selected and sectioned for embedding, because they show a very high organisation of myocardial cells (Fig. 3). The pillars were embedded with four different Θ angles: 0°, 22.5°, 45°, and 67.5°. One image acquisition and one measurement of the mean grey level were made for each pillar of known Θ and Φ angles. Φ angles varied between 0° and 90°, scaled every 11.25° (Fig. 4). Four experimental curves (Fig. 5), each corresponding to a given elevation angle Θ, were fitted to the Johannsen model with the equation $L = \gamma \sin^2(2\Theta) + \eta$, where γ is the constant term corresponding to the elevation angle Θ and η a constant corresponding to the smallest intensity of light, the noise of the camera. Correlation with the theoretical model shows a r^2 superior to 0.99 and is statistically significant with an α value smaller than 0.01.

The 5 values of L obtained with an azimuth angle of 45° were plotted for the monitored Φ angle and compared with the theoretical values obtained with equation 15. The correlation is statistically significant with a r^2 equal to 0.98 and a α value of 0.04. The small deviations from the theoretical model reflect the lack of accuracy of the orientation of the pillars under the objective lens. The tolerance of the positioning was ±2.5°.

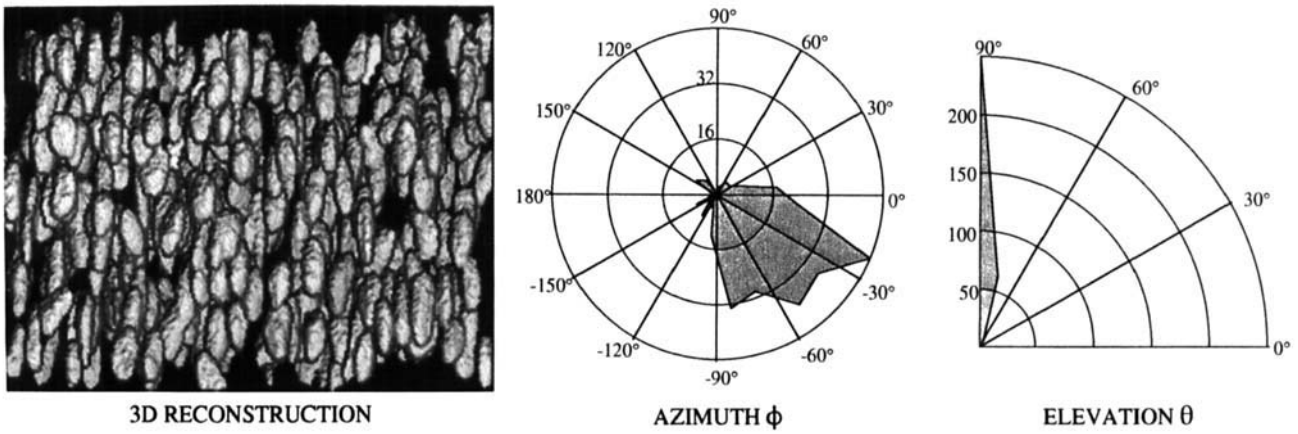

Fig. 3. CSLM analysis: three-dimensional reconstruction of the segmented nuclei for a papillary muscle (**left**). About 300 nuclei have been segmented in a cubic volume 120 μm width. The viewing angle of the reconstruction (orthogonal to the section plane) was selected in order to highlight the degree of organisation of the nuclei. The pillar region shows a very high level of organisation. The diagram of the elevation angle (**right**) shows that the nuclear major axes are mainly oriented orthogonally to the section plane. The diagram of the azimuth angle (**center**) shows a wider distribution, due in part to the ambiguity of definition of an azimuth angle when the elevation angle is almost orthogonal.

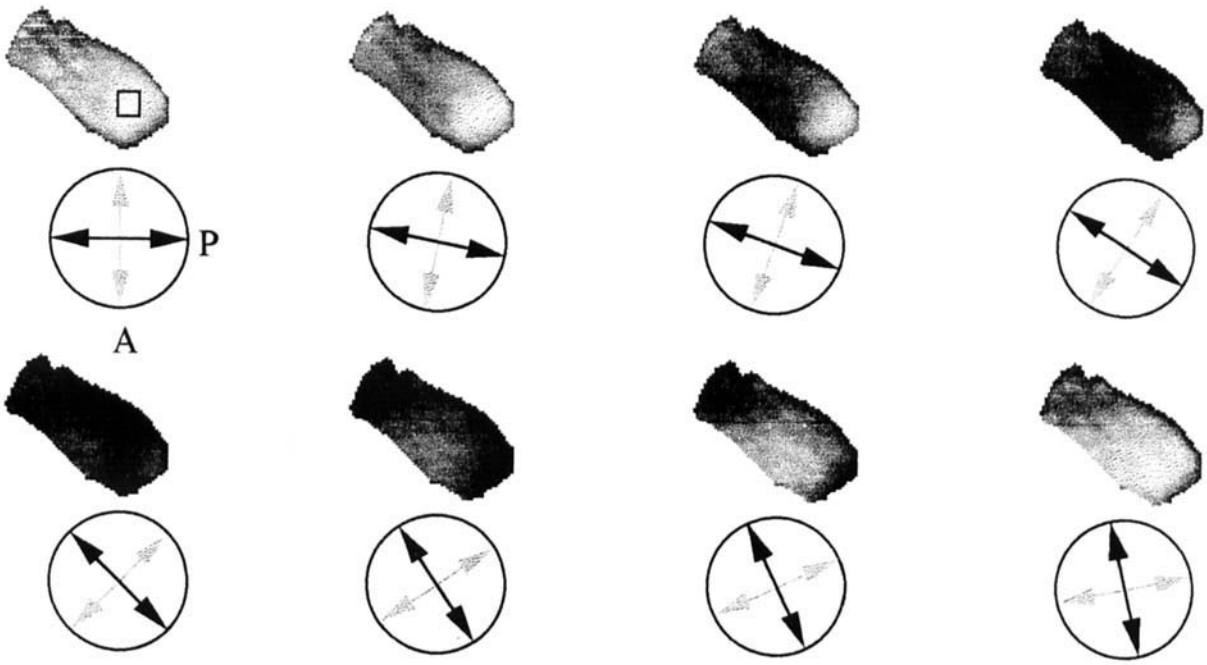

Fig. 4. Polarized light analysis: images of a section of papillary muscle embedded in methylmetacrylate, placed with an azimuth angle of 45°, for eight different configurations of the α angle. From left to right and upper to lower the crossed polars have been rotated from 0° to 78.75° by steps of 11.25°. The black frame on the upper left image shows the sampling area (1 mm × 1 mm) used for the light intensity measurements (see Fig. 5). The arrows in the circles shows the orientation of the axes of the polarizer P (black arrow) and analyzer A (grey arrow)

Validation of Measurement Method

The algorithm has been tested with a hypothetic crystal network with axis radially pointing out and elevation angle Θ rising linearly from periphery to center. We generated four images of polarization of this crystal, each one corresponding to one of the four setups of the α angle, applying the theoretical Johannsen formula 1. These images were used to reconstruct the orientation information with our method. Figure 6a shows the two orientation maps obtained in false colours. The results obtained are consistent with the hypothetical crystal that was generated. The representation of Θ and Φ angles shows continuous variations and no discontinuities.

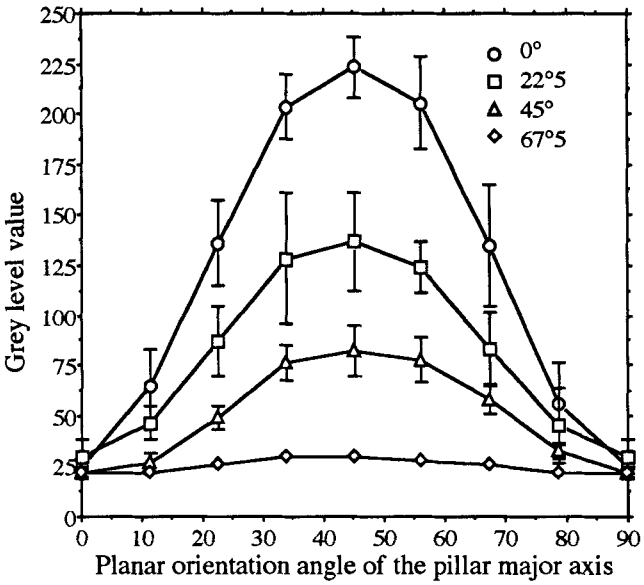

Fig. 5. Polarized light analysis: variation of the amount of transmitted light in papillary muscles. The abcissa correspond to nine different values of the α angle from 0° to 90°, scaled every 11.25° (see Fig. 4). The ordinates correspond to the mean value of the transmitted light; the bars represent the standard deviation. The four curves correspond to four papillary muscles, respectively embedded with an elevation angle Θ of 0°, 22.5°, 45°, and 67.5°.

Mapping of a Fetal Heart Section and Validation by CSLM

Figure 7 shows four images of a section of a fetal human heart at 24 weeks gestation acquired as previously described. These images were analysed, and the resulting cartography is shown Figure 6b.

At the level of the ventricular wall, there is a regular variation of the elevation angle Θ almost orthogonal to the plane of section at the periphery, then gradually decreasing toward the center, where the indicatrix of the myocardium lies horizontally in the plane of the section, and, finally, gradually increasing to become again perpendicular toward the endocardial border of the ventricle. The cartography of azimuth angle shows that Φ mimics the curvature of the ventricular wall.

These data were confirmed by CSLM. The measurement of Θ and Φ made in five zones of the left outer ventricular wall, regularly spaced from the epicardial to the endocardial border (Fig. 8), confirm the data acquired with polarized light (Fig. 9), although some differences can be seen for the elevation angle. The discrepancy observed between angular data (maximum 12°) may be due to two facts: 1) the depth of the sampling area is not the same for CSLM (100 μm) and for polarized light (500 μm); 2) the localization of the two sampled areas in CSLM and in polarized light may not be strictly the same (a variation up to three pixels is possible). These differences were not observed for the azimuth angle, probably because of the low variation of the azimuth in this area.

At the level of the interventricular septum there is a fluctuation of the azimuth between 70° and 90°, while the elevation angle rises gradually from the endocardial border toward the center of the interventricular septum.

At the level of the junctions between the interventricular septum and the ventricular walls, the results reveal the convergence of the circumferentially arranged myocardium into the interventricular septum.

DISCUSSION

The myocardium of fetal and neonatal hearts embedded in methylmetacrylate reacts, when examined between crossed polars, as a positive uniaxial crystal with a 0° extinction angle and very low birefringence. This property allows accurate definition of the 3D orientation of the indicatrix, for each pixel, by multiparametric image analysis. The measures are displayed in the form of two false colour maps: one for the azimuth and the other for Θ the elevation angle, both in the range 0–90°.

Three main points have to be addressed: 1) what are the origins of the birefringence of the myocardium; 2) what are the relationships between the orientation of the indicatrix and the orientation of the other components of the myocardial cells; and 3) what are the limitations of this new technique?

Two main molecules in the myocardium are birefringent: myosin and collagen. The respective amount of each of these molecules is not well known in the fetal and neonatal period. But when compared to the mature heart the volume of the intracellular space, therefore to the contractile proteins, appears more extensive. At the periods studied and in normal heart, the myosin filaments are well organised and aligned along the great axis of the myocardial cells. This volumetric predominance with the relative simplicity of the disposition of myosin filaments and the small size of fetal hearts suggested use of this model, which is a priori simpler than mature or pathologic myocardium. On the other hand, the layout of collagen proteins is more complex, with some fibers aligned along the cells and struts perpendicular to the main axis of the cell. Nevertheless, the positivity of the uniaxial indicatrix confirmed the predominance of molecules longitudinally aligned in the axis of the myocardial fibres.

Although the technique developed here cannot measure the birefringence of the filaments separately in the myocardium, that of the collagen is probably much greater than that of the myosin (Bennet, 1961; Wolman, 1975). The walls of the great vessels which contain a larger amount of collagen are more birefringent than the myocardium. The first consequence for image analysis is that pixels with a birefringence higher than the maximal birefringence of the myocardium have to be discarded from the analysis; otherwise, the determination of the Φ angle would be incorrect. These pixels lie mainly in normal heart in the wall of the great vessels and in pathological hearts in fibroelastosic areas. The second consequence is that image analysis of the whole section relies on the assumption that the respective amount of myosin and collagen is everywhere constant, as in the area sampled for determination of maximal birefringence. Indirect correlation by means of CSLM shows the likelihood of this assump-

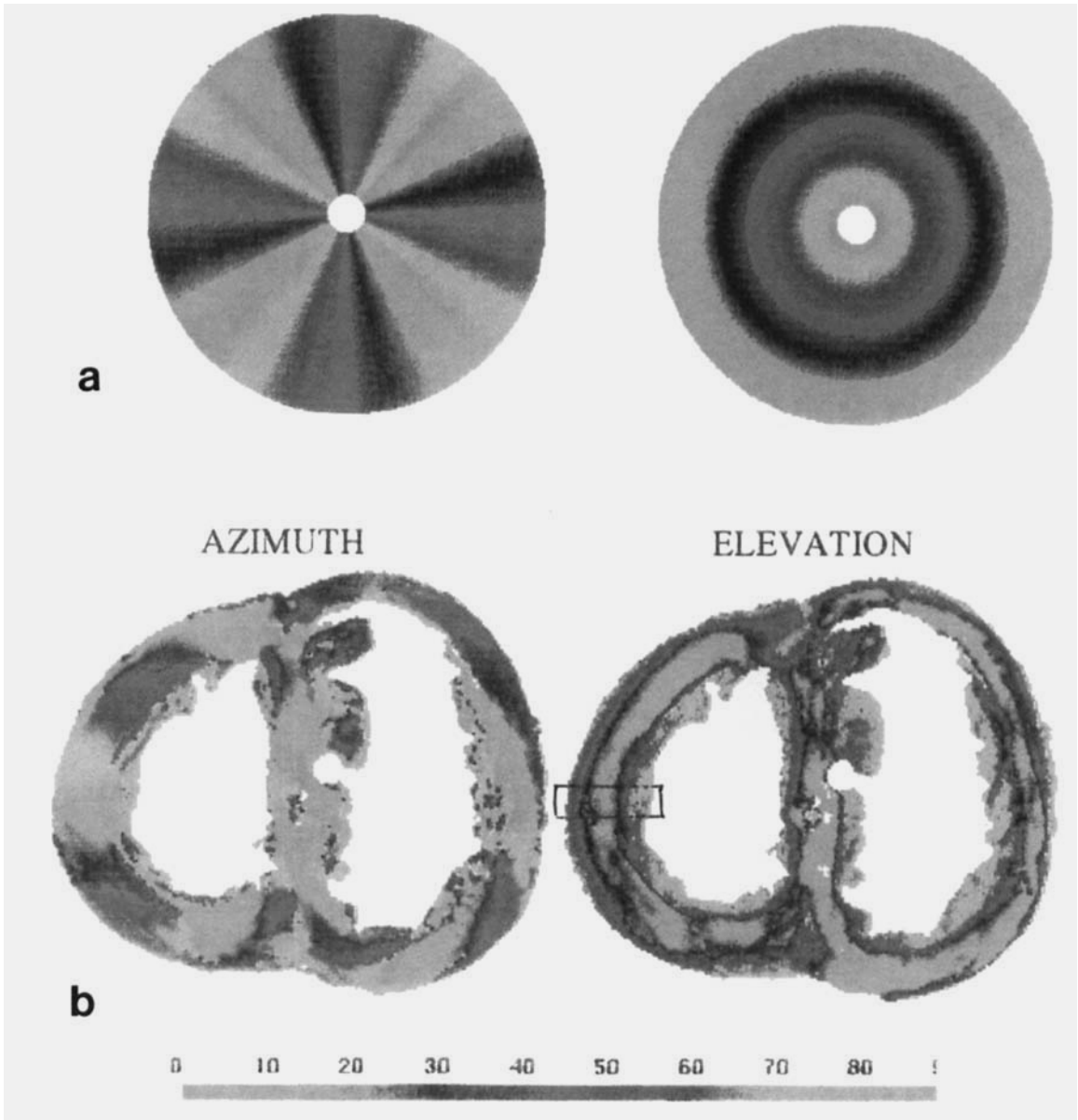

Fig. 6. (Figure appears in color in the Color Figure Section immediately following page 490.) **a:** Azimuth map (**left**) and elevation map (**right**) of a hypothetical crystal network whose axis points out radially and the elevation angle Θ rises linearly from periphery to center. The angle values are represented in false colours from red (0°) to green (30°) to blue (60°) and back to red (90°). The black region in the center of the azimuth map corresponds to a region where the Θ angle cannot be obtained because of the lack of resolution of dynamic (256 grey levels). The same observation can be made for the elevation map where obliquities greater than 75° cannot be revealed. **b:** Polarized light analysis: azimuth map (**left**) and elevation map (**right**) of the same section of a fetal human heart as in Fig. 7. The angle values are represented in false colors from red (0°) to green (30°) to blue (60°) and back to red (90°). The black line drawn on the external wall of the left ventricle azimuth map shows the sampling area for CSLM analysis. The A, B, C, D, and E points, referred to in Fig. 8, are regularly spaced along this line from the outer side to the inner side of the ventricular wall.

tion in the normal heart. But in the pathological heart the deviation of the pattern of the elevation angle map has to be studied. However, it must be considered that such a variation may also exist or alternatively is the consequence of a variation of the respective amount of myosin and collagen.

Another potential cause of variation in the cartography of the elevation angle is the heterogeneity of the sarcomere length all over the heart. This can result in a 5 to 7% change in the measured intrinsic birefringence of the muscle (Taylor, 1975, 1976), but the resultant variation of the value of Φ is less than 1°.

There is another limitation to our present technique. As shown in Figure 5, there is a lack of resolution of

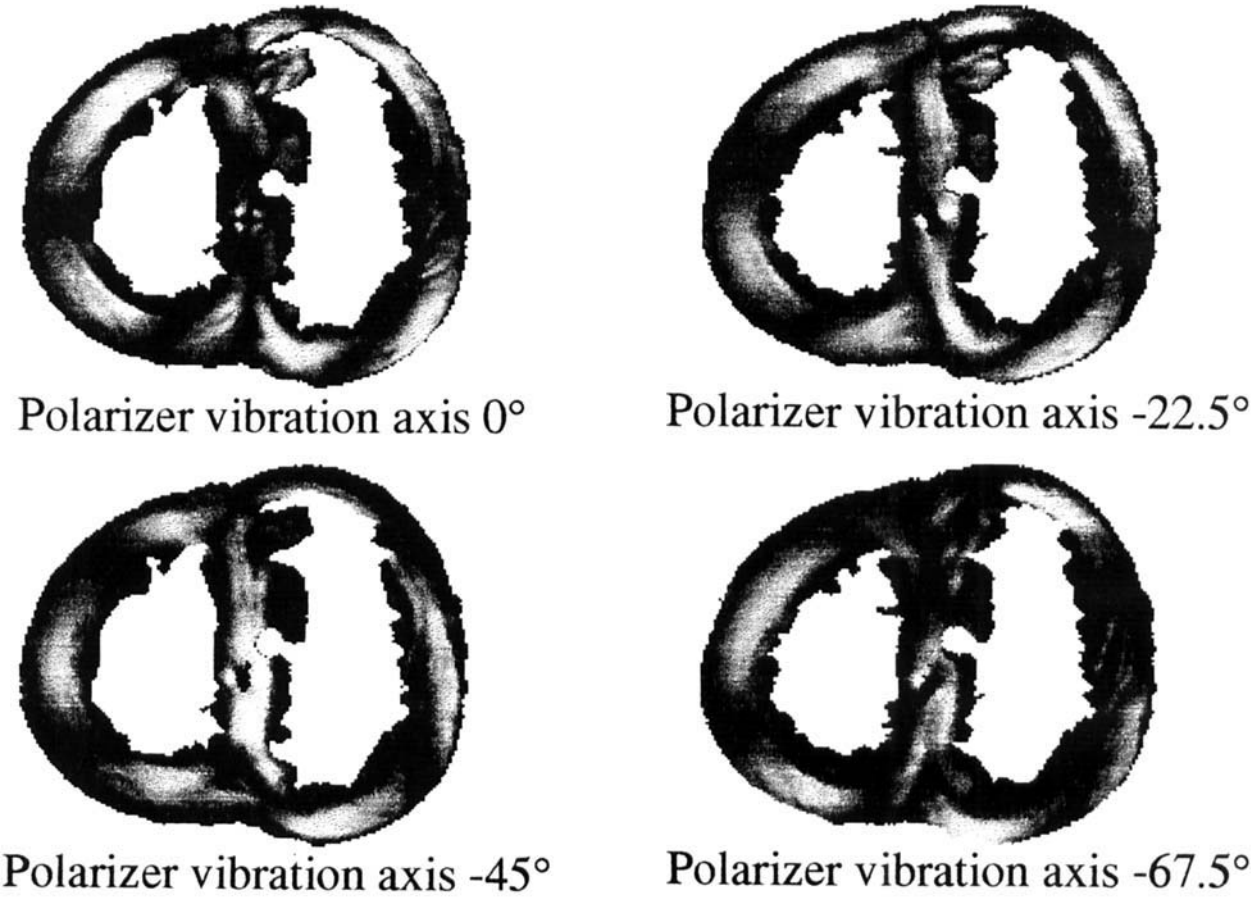

Fig. 7. Polarized light analysis of a thick section of a 24 week gestation human fetal heart. Each image of the section was made with a different setup of the α angle: polarizer vibration axis 0°, −22.5°, −45°, and −67.5°.

grey level dynamics which does not permit discrimination between the different values of the elevation angle lying in the class 75–90° and for the azimuth angle corresponding to these high values of Θ. This is due on the one hand to the rapid variation of the angle Θ for the lowest value of L given by equation 15 and on the other hand to the fact that the measurements of light intensity are encoded with 256 grey levels (8 bit digitizing scale)—that is, the angles between 75° and 90° are coded with only one grey level. This limitation could be theoretically alleviated by coding the data with 4,096 grey levels (12 bits). This would require different hardware, presently far more expensive.

Polarized light analysis gives information on the three-dimensional orientation of the indicatrix of the myocardium. As previously discussed, the orientation of the indicatrix is relevant to the orientation of the main birefringent molecules of the myocardium. In normal heart, our study showed the good correlation between the orientation of the great axis of the nucleus studied by CLSM and the orientation of the indicatrix. However, it is not always the case: in some myocardial disarray, the orientations of the nuclei diverge from the orientations of the myofibres. Therefore, to fully characterize myocardial disarray, it is necessary to specify the two characteristics: orientation of the indicatrix and orientation of the nuclei.

In another field, multiparametric analysis of polarized light has already been used by Guido and Tranquillo (1993). They studied the orientation of collagen fibres in a contact guidance prepared three-dimensional gel. In their methods, the measurement of the grey level was done for α values varying from 0–180° by steps of 5°. The sample was placed on a rotating stage, while the polarizer and the analyser remained motionless. Thus the position of each pixel of the image has to be calculated for each setup of the α angle in order to establish the curve of the variation of the grey level value. Finally, the gel birefringence was correlated with the homogeneity of the orientation of the collagen fibres without trying to discriminate between variations in the azimuth angle and the elevation angle. The method described in the present paper is a significant improvement for the study of the orientation of birefringent molecules. The adaptation of the microscopical stage makes it possible to keep the sample motionless; this results in a simpler and more accurate way to study the variation of the grey level val-

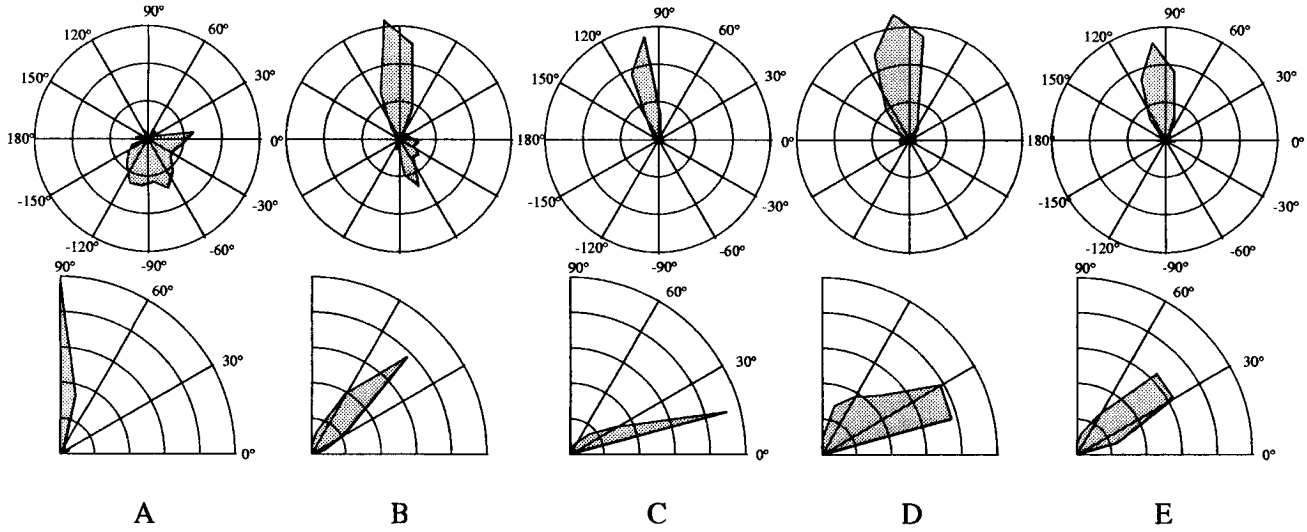

Fig. 8. CSLM analysis: diagram of the azimuth (**upper**) and elevation angle (**lower**) of the volumes sampled through the left ventricular wall. **A:** Outer side. **B:** Junction between outer quarter and middle outer quarter. **C:** Middle. **D:** Junction between middle inner quarter and inner quarter. **E:** Inner side (Fig. 6). Upper: The 0–180° axis corresponds to the x line perpendicular to the interventricular septum. Lower: 0° refers to the section plane (parallel to the plane of the atrioventricular valves).

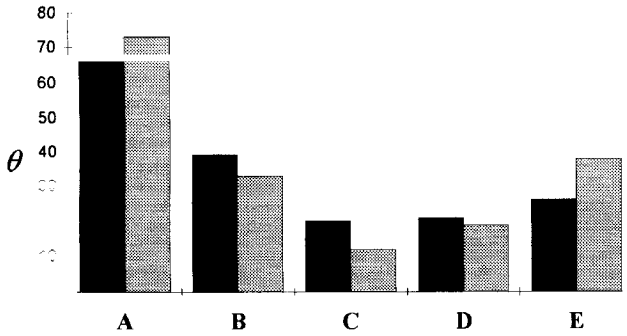

Fig. 9. Histogram of the elevation angle Θ of five volumes sampled through the ventricular wall. **A:** Outer side. **B:** Junction between outer quarter and middle outer quarter. **C:** Middle. **D:** Junction between middle inner quarter and inner quarter. **E:** Inner side. Black bar: Elevation angle measured with confocal scanning laser microscopy. Grey bar: Elevation angle measured with polarized light.

ues as a function of α. It also shows that four acquisitions every 22.5°, instead of 36 every 5°, are sufficient to extract the complete information on the three-dimensional orientation of the birefringent molecules. We have shown that multiparametric image analysis with polarized light makes it possible to accurately define the elevation angle Θ.

Other attempts had been made to define this elevation angle, which relied essentially on the use of polarized light and an universal stage (Canham et al., 1986; Smith et al., 1981). These studies were derived from geological methods (Emmons, 1943). But their direct application to biological material is awkward. Indeed, their goals are different. The main purpose in geology is the identification of minerals. Thus, usually a very small sample of the mineral is selected because of its regularity and the main properties to be measured: birefringence and extinction angle. In biology, the networks are less regular, and the main purpose is to study the variation of the orientation of the birefringent molecules. To this end, it is necessary to sample a great deal of the specimen. The universal stage with the numerous handling and movements of slides it requires is not convenient. In contrast, the technique we developed is well adapted to image analysis and automatic acquisition and processing of data. The sample remains stationary. Therefore, by rotating the polar and cross-polar filters to four predefined angles, it is possible to measure for each point of the section the amount of transmitted light. It is the combination of these measurements which makes it possible to discriminate between the variation of transmitted light due to the azimuth angle and to the elevation angle. With the present method the azimuth angle ϕ is known modulo 90°. This is the main limitation of the method which presently precludes giving a complete three-dimensionnal representation of the orientation of the indicatrix of the myocardium. We are presently working out a way to solve this problem. It is based on the use of a first order λ retardation plate that provides useful chromatic information. The spectral analysis of this information will make it possible to extend the range of measurement to the full 0–180° scale.

This work was supported by the Association Française de lutte contre les Myopathies (AFM-90,91,92) and the Fondation pour la Recherche Médicale (FRM 92). The authors thank Dr. Victoria von Hagen for her advice in editing the manuscript, Mr. Gandini (Ecole Française de Papeterie et Arts Graphiques) and Mr. Barbier (Elf-Atochem) for their

expert advice on chemistry, Mr. Christin (Atelier de spectrométrie physique) for manufacturing the microscopical stage, and Mrs. Grossi for excellent technical help.

REFERENCES

Batschelet, E. (1981) Circular Statistics in Biology. Academic Press, London, pp. 214–219.

Bennet, H.S. (1961) Methods applicable to the study of both fresh and fixed materials. The microscopical investigation of biological materials with polarized light. In: McClung's Handbook of Microscopical Technique. New York, Hafner, pp. 591–677.

Canham P.B., Finlay, H.M., Whittaker, P., and Starkey, J. (1986) The tunica muscularis of human brain arteries: Three-dimensional measurement of alignement of the smooth muscle mechanical axis, by polarized light and the universal stage. Neurol. Res., 8:66–74.

Emmons, R.C. (1943) The universal stage. Geol. Soc. Am. Mem., 8:1–205.

Fox, C.C., and Hutchins, G.M. (1972) The architecture of the human ventricular myocardium. Hopkins Med. J., 130:289–299.

Frey-Wyssling, A. (1957) Macromolecules in Cell Structure. Harvard University Press, Cambridge, MA.

Greenbaum, R.A., Ho, S.Y., Gibson, D.G., Becker, A.E., and Anderson, R.H. (1981) Left ventricular fibre architecture in man. Br. Heart J., 45:248–263.

Guido, R., and Tranquillo, R.T. (1993) A methodology for the systematic and quantitative study of cell contact guidance in oriented collagen gels. Correlation of fibroblast orientation and gel birefringence. J. Cell Sci., 105:317–331.

Hort, W. (1960) Makroskopische und mikrometrische untersuchungen am myokard verschieden stark gefüllter linker kammern. Virchows Arch. Pathol. Anat., 33:523–564.

Johannsen, A. (1918) Manual of Petrographic Methods. McGraw-Hill, New York, 649 pp.

Maron, B.J., and Roberts, W.C. (1979a) Quantitative analysis of cardiac muscle cell disorganization in the ventricular septum of patients with hypertrophic cardiomyopathy. Circulation, 59:689–706.

Maron, B.J., and Roberts, W.C. (1979b) Quantitative analysis of cardiac muscle cell disorganization in the ventricular septum. Comparison of fetuses and infants with and without congenital heart disease and patients with hypertrophic cardiomyopathy. Circulation, 60:685–696.

Maron, B.J., Anan, T.J., and Roberts, W.C. (1981) Quantitative analysis of cardiac muscle cell disorganization in the left ventricular wall of patients with hypertrophic cardiomyopathy. Circulation, 63: 882–894.

McLean, M.R., and Prothero, J. (1987) Coordinated three-dimensional reconstruction from serial sections at macroscopic and microscopic levels of resolution: The human heart, Anat. Rec., 219:434–439.

McLean, M.R., and Prothero, J. (1991) Three-dimensional reconstruction from serial sections. V. Calibration of dimensional changes incurred during tissue preparation and data processing. Anal. Quant. Cytol. Histol., 13:269–277.

Parazza, F., Humbert, C., and Usson, Y. (1993) Method for 3D volumetric analysis of intranuclear fluorescence distribution in confocal microscopy. Comput. Med. Imaging Graph., 17:189–200.

Pickering, J.G., and Boughner, D.R. (1990) Fibrosis in the transplanted heart and its relation to donor ischemic time. Assesment with polarized light microscopy and digital image analysis. Circulation, 81:949–958.

Ruthman, A. (1970) Methods in Cell Research. C. Bell and Sons, London.

Smith, J.F.H., Canham, P.B., and Starkey, J. (1981) Orientation of collagen in the tunica adventitia of the human cerebral artery measured with polarized light and the universal stage. Ultrastruct Res., 77:133–145.

Streeter, D.D. (1979) Gross morphology and geometry of the heart. In: Handbook of Physiology, Vol. 1. Williams and Wilkins, Baltimore, pp. 61–112.

Taylor, D.L. (1975) Birefringence changes in vertebrate striated muscle. J. Supramol. Struct., 3:181–191.

Taylor, D.L. (1976) Quantitative studies on the polarization optical properties of striated muscle. I. Birefringence changes of rabbit psoas muscle from rigor to relaxed state. J. Cell Biol., 68:497–511.

Torrent-Guasp, F. (1973) The Cardiac Muscle. Fundaciòn Juan March, Madrid.

Usson, Y., Parazza, F., Jouk, P.-S, and Michalowicz, G. (1994) Method for the study of the three-dimensional orientation of myocardial cells by means of confocal scanning laser microscopy. J. Microsc., 174:101–110.

Whittaker, P., Romano, T., Silver, M.D., and Boughner, D.R. (1989) An improved method for detecting and quantifying cardiac muscle disarray in hypertrophic cardiomyopathy. Am. Heart J., 118:341–346.

Whittaker, P., Boughner, D.R., and Kloner, R.A. (1989) Analysis of healing after myocardial infarction using polarized light microscopy. Am. J. Pathol., 134:879–893.

Wolman, M. (1975) Polarized light microscopy as a tool of diagnostic pathology. J. Histochem. Cytochem., 23:21–50.